



Regular Research Manuscript

## Sediment Characteristics and Hydrocarbon Composition of Makukwa Seep in Southern Tanzania: Potential Implications for Subterranean Hydrocarbon Accumulation

Claude A. Mosha, Makungu M. Madirisha\*, Kessy F. Kilulya, and Esther H. J. Lugwisha

Chemistry Department, University of Dar es Salaam, P.O. Box 35061, Dar es Salaam, Tanzania

\* Author corresponding email: [makungu.madirisha@udsm.ac.tz](mailto:makungu.madirisha@udsm.ac.tz)

ORCID: <https://orcid.org/0000-0002-4037-3974>

### ABSTRACT

*Exploring the interplay between natural seeps and nearby sediment and hydrocarbon properties is key to unlocking subsurface hydrocarbon potential. This study presents findings on the hydrocarbon composition and sediment characteristics of the Makukwa seep in southern Tanzania, providing insight into subterranean hydrocarbon accumulation. Sediment analysis across areas A and B, located approximately 20 m apart, showed a decrease in porosity with depth, indicative of typical sandstone formations. Area A, near the seeps, exhibited porosity ranging from 23% to 36%, whereas Area B, further away, showed porosity ranging from 22% to 38%. This suggests that a lower cretaceous sandstone layer may have overlain the hydrocarbon seep. XRD analysis confirmed quartz as the dominant mineral, with concentrations of 46.1% in area A and 50.1% in area B, underscoring the sediment's sandstone-like nature. Additionally, graphite was higher in area A (29.5%) than in area B, indicating a varying degree of hydrocarbon influence across the sampled locations. ICP-OES analysis revealed elevated trace metal concentrations, particularly iron, which varied from 27.47 ppm to 471.47 ppm in area A, significantly higher than in area B, indicating the geochemical influence of hydrocarbon seepage on sediment composition. GC-MS analysis showed a range of heavy aliphatic hydrocarbons (n-alkanes) from n-C14 to n-C38 within the sediments, indicating a dormant state. Notably, the concentrations in area A were higher, with specific hydrocarbons such as octadecane and eicosane measured at 0.330 µg/mL and 0.789 µg/mL, respectively, compared with the lower concentrations in area B (octadecane at 0.105 µg/mL and eicosane at 0.089 µg/mL). This highlights the impact of proximity to the seep on hydrocarbon distribution. This study offers crucial insights into hydrocarbon dynamics at the Makukwa seep, Tanzania, highlighting the relationship between sediment properties and hydrocarbon accumulation. These findings enhance our understanding of hydrocarbon seepage, guiding future exploration and environmental monitoring efforts.*

### ARTICLE INFO

Submitted: **Jan. 23, 2024**

Revised: **March. 12, 2024**

Accepted: **Apr. 3, 2024**

Published: **Apr., 2024**

**Keywords:** Hydrocarbon, Makukwa seep, Porosity, Sediment, Subsurface hydrocarbon accumulation and Trace metal ions.

## INTRODUCTION

Oil or gas seepages have been instrumental in discovering many commercial oil and gas fields in both new and established basins (Boruah et al., 2022). 81% of geological methane seepages occur in petroleum fields while the remaining 19% are attributed to smaller petroleum reservoirs or long-distance migration from source rocks (Ciotoli et al., 2020). Hydrocarbon seeps, which occur both on the seafloor and on land, represent critical natural pathways for hydrocarbons from subsurface reservoirs to reach the surface (Techtmann et al., 2015). These phenomena are a common feature across the globe's oil basins, with the notable exception of areas possessing intact, unfractured seals (Joye, 2020; Schumacher and Foote, 2014). The presence of

hydrocarbon seepage serves as a direct marker for subsurface hydrocarbon accumulations, shedding light on the processes of hydrocarbon migration within sedimentary basins (Kleindienst et al., 2012). Not only do these seeps provide valuable geological insights, but they also form distinct geomorphological structures offshore, such as gas bubbles (**Figure 1**) and mud volcanoes alter the chemical compositions of onshore and sediments (Cochran et al., 2022; Ionescu et al., 2017). These alterations, impacting clay and non-clay minerals of varying permeability and porosity, highlight the economic importance of hydrocarbon seeps in the preliminary phases of petroleum exploration, marking them as focal points for investigative efforts (Almeida-Filho et al., 1999; Dupré et al., 2010).

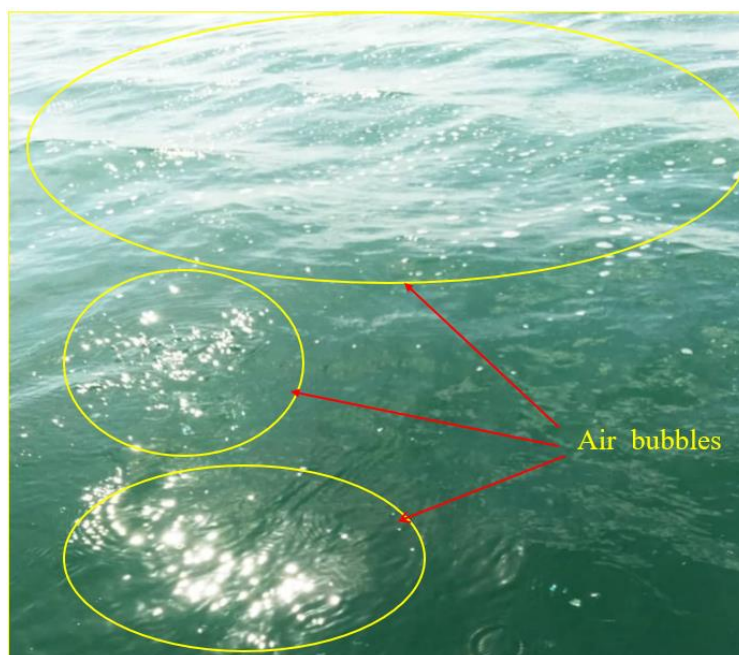


**Figure 1: Ipwalapwata gaseous hydrocarbon seep, located in the Indian Ocean near the Makukwa village in Mtwara region, Tanzania (Photo courtesy: Mzee Juma from Makukwa Village).**

Hydrocarbon seeps are often dominated by methane seepage with minor concentrations of other hydrocarbon gases (Kleindienst et al., 2012). They are commonly associated with mud volcanism, gas emissions, and the precipitation of authigenic carbonates, providing habitats

for unique chemosynthetic life forms (Dupré et al., 2010). The geological processes responsible for seeping activities and the biogeochemical processes related to them have been studied using various techniques such as seismic recordings, coring, and genomic analysis (Li et al., 2021). Additionally, the distribution of

hydrocarbon seeps is influenced by tectonic settings, with seeps prevailing in convergent basins and along brittle tectonic structures (Ciotoli et al., 2020).

Hydrocarbon seeps are found in both marine and terrestrial environments, with some regions like the Eastern Mediterranean containing numerous active seeps (Teichtmann et al., 2015). These seeps are crucial markers of hydrocarbon migration and are linked to the presence of sulfate-reducing bacteria in marine sediments (Kleindienst et al., 2012). The study of hydrocarbon seeps provides valuable information for understanding geological processes, biogeochemical cycles, and the distribution of unique ecosystems in cold seep environments (Dong et al., 2024). To elaborate, hydrocarbon seeps can either emanate from biogenic or thermogenic processes (Abrams, 2005; Boruah et al., 2022; Cochran et al., 2022). Where, biogenic seeps result from the metabolic activities of bacteria, while thermogenic seeps emerge from the transformation of organic materials under high temperatures deep within the subsurface (Ciotoli et al., 2020). These seeps, often marked by low pressure,

exhibit a slow release of varied compositions including gases, crude oil, liquid bitumen, asphalt, and tar (Clark et al., 2010; Ward et al., 2017). Understanding these compositions is pivotal for identifying subsurface hydrocarbon types and refining exploration strategies, such as drilling. Additionally, the mineralogical composition of sediments near hydrocarbon seeps critically influences their porosity and permeability, which are key factors in assessing hydrocarbon volumes and flow rates of seepage (Cather et al., 1991; Lelfer et al., 2014). This knowledge is instrumental in guiding the exploration and evaluation of hydrocarbon deposits.

Tanzania's seismic data have revealed significant oil and gas reserves, primarily located across its varied sedimentary basins (Muhongo, 2013a; Muhongo, 2021; Muhongo, 2013b; Rachel Angelo et al., 2019). As depicted in **Figure 2**, these basins are classified into four main categories: inland rift basins, coastal basins, shelf and shallow offshore basins, and deep offshore basins (Muhongo, 2013b; Rachel Angelo et al., 2019).

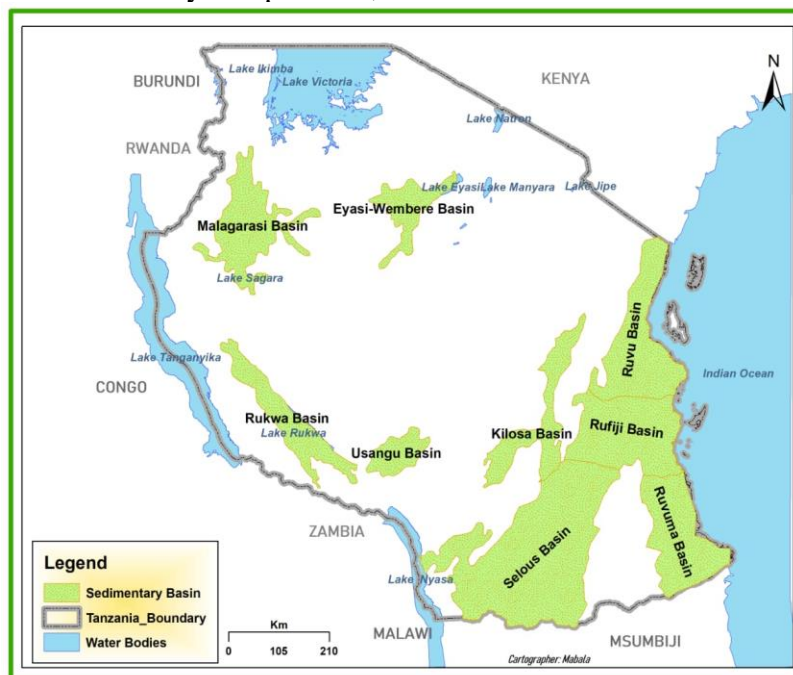


**Figure 2:** A Map of Tanzania showing the distribution of sedimentary basins (Muhongo, 2013b; Rachel Angelo et al., 2019; TPDC, 1992).

This classification underscores the geological variety and potential resource richness of the region, guiding exploration, and development strategies for Tanzania's hydrocarbon resources.

## METHODS AND MATERIALS

### Experimental Work

#### Study Area

The Makukwa hydrocarbon seep is located in Mtwara district (**Figure 3**) within the Ruvuma

sedimentary basin, which is a major East (E)-West (W) trending basin in the coastal area of Tanzania along the passive continental margin of the western Indian Ocean. It borders the Mandawa Basin to the southeast, the Selous Basin to the southwest, and the Ruvu Basin to the North. Makukwa hydrocarbon seep is believed to have potential for hydrocarbons but remains significantly unexplored. It covers an area of approximately 16,000 sq. km 200 km westward from the coastline to the Ulanga basement spur.

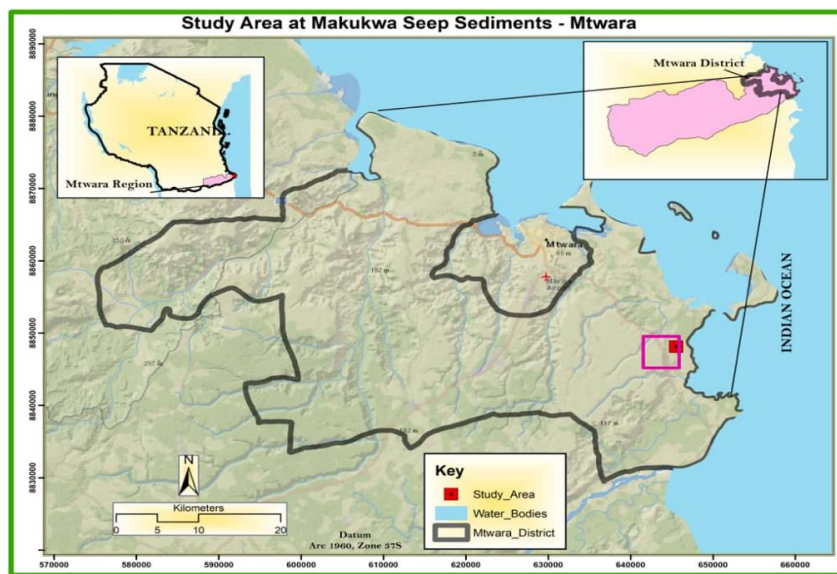


**Figure 3: Map of Mtwara district showing Makukwa hydrocarbon seep as a sampling site (map courtesy: Zakaria E. Mabala)**

#### Sample Collection

Sediment samples were systematically gathered from the Makukwa hydrocarbon seep following the methodology outlined by Bohrmann (2008). The site was divided into two distinct sampling zones: Area A, close to the seeps, and Area B, situated further away. Each zone was subdivided into nine blocks of four-square meters each. Six of these blocks were randomly chosen from each zone to serve as the sampling sites. This selection strategy facilitated the collection of a manageable and representative subset of samples, ensuring comprehensive coverage across varying sections of the sampling zones. Consequently, the remaining three blocks in each area were excluded from the sampling

process. At each site, six samples were extracted in triplicate across depths ranging from 0.5 meters to three meters. In total, 72 samples were collected using an auger, then sealed in plastic bags and preserved in plastic containers for analysis.

#### Sample preparation

Sediment samples were prepared according to the standard operating procedures for preparing soil/sediments (Carter and Gregorich, 2007; USEPA, 2016). To prevent cross-contamination, each wet sediment sample was transferred onto clean glass slides using separate spatulas. The samples were then oven-dried at 120 °C for two hours to eliminate moisture content. This drying step, which follows a protocol modified from Belzunce Segarra et al. (2007), ensures that

moisture is effectively removed without harming temperature-sensitive substances. After drying, the samples were cooled in desiccators for 15 minutes. This method maintains the integrity of the samples for reliable subsequent analyses, including chemical extraction and metal determination. Precisely, the specified temperature and time strike a balance between efficiency and safety, preserving the chemical integrity of organic compounds within the samples. The dried samples were then ground in a mortar and pestle to obtain uniform-sized samples with increased surface areas for ease and effective extraction for subsequent metal determination. The optimal magnitude of force for grinding sediment samples was typically determined through several trials. These trials helped to establish a balance where the particle size was adequate for the intended analyses without causing contamination or excessive alteration of the sample. The sediment samples were subjected to wet acid digestion using aqua regia (nitrosyl chloride) by freshly mixing concentrated hydrochloric and nitric acids. The digest was filtered through Whatman filter paper on a funnel into a 100 mL volumetric flask and diluted with distilled water to the mark.

To ensure the reliability of the metal determination process using Inductively Coupled Plasma Optical Emission Spectrometry (ICP-OES), procedural blanks were meticulously prepared. These blanks are essential for identifying and correcting any background contamination and instrumental biases. They were processed identically to the sediment samples, minus the addition of sediment, to serve as a baseline for comparison. This step was critical for the accurate quantification of trace metals—iron (Fe), manganese (Mn), chromium (Cr), zinc (Zn), nickel (Ni), copper (Cu), cadmium (Cd), arsenic (As), and lead (Pb)—in the samples, ensuring that the measurements reflect only the metals present in the sediments and not contaminants from the preparation process. Each of the prepared 100 mL digested sediment solutions was then aliquoted, with

25.0 mL transferred into clean polyethylene bottles, ready for the precise determination of trace metals, marking a comprehensive approach to sediment sample preparation and analysis.

### **Extraction of Hydrocarbons**

Hydrocarbons from the samples were extracted using the Soxhlet extraction method as per Environmental Protection Agency (EPA) 3540 C (USEPA, 2016). About 30 g of the sample was mixed with sodium sulfate to remove any water molecules in the sample and then placed in the extraction thimble. The sample was then extracted with 100 mL of hot toluene for 20 hours. The extract was then placed in the water bath conditioned at 40 °C to evaporate the solvent and concentrate the hydrocarbons.

### **Characterization of Sediments and Hydrocarbons**

Particle size distribution and porosity of sediment samples from sampling areas A and B were determined using two key methods, namely, sieving and volumetric water displacement, respectively. For particle size distribution, the dried original samples (non-crushed) were sieved to separate the sediments into fractions depending on their particle sizes. Size fractions were separated as 4750 µm, 3350 µm, 2360 µm, 1700 µm, 1180 µm, 850 µm, 600 µm, 425 µm, 300 µm, 212 µm, 150 µm, 75 µm and < 75 µm. About 100 mL of water was measured using a measuring cylinder and poured into the testing cup for porosity. The water level in the testing cup was marked, and water was poured back into the measuring cylinder. The marked testing cup was filled with the sample (sediment) up to the mark. Water from the graduated cylinder was poured slowly into the sediments until the water level just reached the top of the sediments. The amount of water left in the graduated cylinder was recorded and subtracted from the original 100 mL to obtain the volume of the pore space. Porosity was calculated using Equation 1.

$$\text{Porosity} = \frac{\text{Pore space volume}}{\text{Total volume}} \times 100\% \quad (1)$$

For the chemical composition of sediments (phase composition), the XRD analysis was performed using Bruker X-ray diffraction XRD. The analysis was performed using Cu K $\alpha$  X-rays ( $\lambda = 1.541874 \text{ \AA}$ ) over the  $2\theta$  range from 5.001 to 64.997 degrees in the steps of 0.02 ( $2\theta$ ) degree in continuous scanning mode at room temperature. The generated XRD data were interpreted using MATCH software for phase identification. For hydrocarbon composition, Gas Chromatography-Mass Spectrometry (GCMS-2010 Shimadzu instrument) operating in Electron Ionization (EI) mode (MS) at 70 eV. A Restek-5MS column (30m x 0.25mm x 0.25 $\mu$ m) was used. The oven temperature program was 90 °C to 300 °C and held at 90 °C for two minutes. The temperature was then increased to 300 °C for 4 minutes (hold time) at 4 °C per minute. The injection temperature was 250 °C with split injection mode. The flow rate of carrier gas helium was set at 1.21 mL/min. The ion source temperature and interface temperature in MS were 230 °C and 300 °C, respectively. The identification of hydrocarbons in the samples was performed using the scan method, which used a Mass Spectral Library and Search Software (NIST 11). Hydrocarbons in the samples were quantified using the Peak Integration method whereby ion allowance was 20%, target ion, and other five references (quantitation) ions were used in quantitative analysis. 20  $\mu$ L of the sample was injected in dichloromethane to make 1 mL and then injected in GC MS. Identification of hydrocarbons was done by comparing retention times and mass spectra of the analytes to those of the reference standards run concurrently and at the same conditions with the samples.

Determination of the physical and chemical properties of the extracted hydrocarbons was performed using American Standards test methods (ASTM). The analyzed properties include sulfur content, ash content, and carbon residual. Sulfur, ash and carbon

residual content were measured using ASTM 4294, 482 and 189, respectively.

## RESULTS AND DISCUSSION

### RESULTS AND DISCUSSION

#### Volumetric Water Displacement and Sieving Results: Porosity and Particle Size Distribution

The porosity of sediment samples from sampling areas A and B, as indicated in **Table 1** and **Table 2**, respectively, showed mean values ranging from 24% to 36% and 23% to 38%. These porosity ranges fall within the typical porosities observed in hydrocarbon formations, such as lower Cretaceous sandstone formations (Japsen et al., 2007; Lahiri et al., 2022). The decrease in average porosity with increasing sediment depth can be attributed to enhanced compaction and grain packing as depth increases. This phenomenon is commonly observed as grain sizes decrease with depth, leading to a reduction in void spaces and subsequently lowering the overall porosity of the sediments (Lahiri et al., 2022; Lai et al., 2018). These findings are further supported by existing literature, which indicates that porosity diminishes exponentially with depth due to compaction. Increased burial depth alters the initial packing of sediments, resulting in reduced pore volume as compaction progresses (Wang et al., 2019). Additionally, porosity is intricately linked to sediment grain characteristics, including size, shape, grading, and packing, as well as the initial consolidation process. Laczko-Dobos et al. (2020) and Wang et al. (2019) further emphasized that deep-burial diagenetic processes play a crucial role in controlling porosity development in sandstones, especially in lacustrine environments. In general, the porosity of sediment samples is crucial for understanding their hydrocarbon potential, with lower porosities at greater depths due to compaction processes altering grain packing and reducing pore volume. These findings align with the established

geological principles and studies on porosity evolution in sedimentary formations. Particle size distribution (PSD) results are presented in Figure 4. The mean percentage of PSD ranged from 0 - 86.21% for sediment samples in area A and 0-100% for samples in

sampling area B. The maximum percentage of PSD was obtained in a sieve size of 4750  $\mu\text{m}$ , which reflects a sandstone grain size. Taking this into consideration, the results, therefore, agree with the obtained mean porosity and further typify the sandstone formation.

**Table 1: Porosity (%) of Sediments from Sampling Area A**

Depth (m)	% Porosity of Sediment						Mean $\pm$ SD
	A_1	A_2	A_3	A_4	A_5	A_6	
0.5	37	42	37	29	36	36	36 $\pm$ 4
1	35	37	34	27	30	33	33 $\pm$ 4
1.5	28	22	30	27	26	30	27 $\pm$ 3
2	28	22	28	24	26	28	26 $\pm$ 3
2.5	28	21	24	22	24	26	24 $\pm$ 3
3	22	21	20	22	24	26	23 $\pm$ 2

**Table 2: Porosity (%) of Sediments from Area B**

Depth (m)	% Porosity of Sediment						Mean $\pm$ SD
	B_1	B_2	B_3	B_4	B_5	B_6	
0.5	41	22	40	31	30	32	38 $\pm$ 7
1	37	22	35	31	28	32	31 $\pm$ 5
1.5	30	22	31	29	28	28	28 $\pm$ 3
2	26	21	28	28	23	28	26 $\pm$ 3
2.5	20	22	21	28	20	28	23 $\pm$ 4
3	18	22	21	25	20	27	22 $\pm$ 3

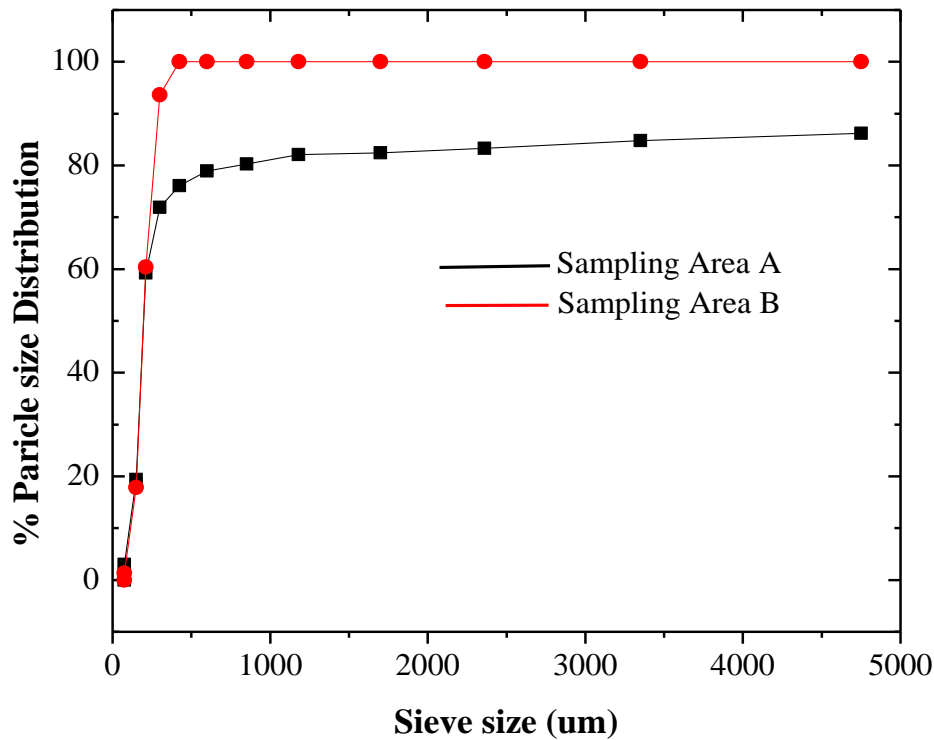


**Figure 4: Particle size distribution in Sampling Area A and Sampling Area B as determined by sieve analysis.**

#### ICP-OES results of trace metal Ions

Trace metal concentrations (ppm) in sediment samples of the study area are presented in **Tables 3** and **4**. It was observed that the concentrations of some trace metals were tremendously increased in sampling area A, which is close to the seep, compared to those in sampling area B, which is far from the seep. This notable increase is likely attributed to the uptake of trace metals from aqueous or mineral phases during the primary and secondary migration of hydrocarbons during seepage events. The hydrocarbon seepage likely induced a reducing environment, enhancing the solubility of trace metals and facilitating their transportation and deposition in the sediments (Boruah et al., 2022). Recent studies have corroborated these findings, showing anomalous concentrations of trace elements in sediments near hydrocarbon seeps, with a wide range of concentrations for various metals (Boruah et al., 2022). Additionally, the presence of a reducing environment near seepage areas has been linked to increased metal concentrations in sediments, as observed in studies focusing on hydrocarbon seep sediments (Mishra et al.,

2020). The transport and deposition of trace metals in sediments near seepage zones are influenced by various factors, including the geochemical characteristics of the sediments and the nature of the seepage processes (Luo et al., 2022).

Based on the correlation analysis of the concentration of trace metals in the sediment samples with depth, the results showed that the concentration of trace metals increased with depth in the following order; Fe > Mn > Zn > Cr > Ni > Cu > As > Pb > Cd for sampling area A while for sampling area B the order was Fe > Mn > Cu > Zn = Cr = Ni = Cu = As = Pb = Cd. Fe and Mn showed the maximum increase in both sampling areas, and this might be due to increased amounts of soluble Fe and Mn in the reducing environment caused by the seepage of hydrocarbons. According to (Rasheed et al., 2013), metals become more soluble in reducing environments, hence, the elevated levels of trace metals, higher than their average concentrations observed in sediments, indicate hydrocarbon-induced alterations in the area.

Overall, these findings highlight the significant influence of hydrocarbon seepage on trace metal concentrations in sediments and underscores the value of these geochemical anomalies in hydrocarbon exploration. The elevated levels of trace metals, higher than their average

concentrations in sediments, indicate hydrocarbon-induced alterations in the area. These results emphasize the importance of incorporating geochemical analyses into exploration strategies to improve targeting accuracy, reduce exploration risks, and enhance overall efficiency.

**Table 3: Mean Concentration of Trace Metal ions (ppm) concerning Depth (m) of Seep Sediments in Sampling Area A**

Mean Concentration of Heavy Metals (ppm)									
Depth (m)	Cu	Zn	As	Pb	Fe	Cd	Mn	Cr	Ni
0.5	0.023	0.257	0.014	0.026	27.47	0.001	0.28	0.509	0.062
1.0	0.031	0.345	0.019	0.033	194.67	0.002	4.89	0.404	0.087
1.5	0.054	0.401	0.051	0.040	206.65	0.009	7.94	0.469	0.213
2.0	0.070	0.507	0.060	0.066	287.48	0.005	4.28	0.527	0.239
2.5	0.094	0.713	0.066	0.048	371.50	0.018	4.65	0.681	0.176
3.0	0.111	0.823	0.083	0.048	471.47	0.014	10.07	0.745	0.137

**Table 4: Mean Concentration of Trace Metal ions (ppm) concerning Depth (m) of Seep Sediments in Sampling Area B**

Mean Concentration of Heavy Metals (ppm)									
Depth (m)	Cu	Zn	As	Pb	Fe	Cd	Mn	Cr	Ni
0.5	0.0007	ND	ND	ND	0.218	ND	0.009	ND	ND
1.0	0.001	ND	ND	ND	0.237	ND	0.008	ND	ND
1.5	0.002	ND	ND	ND	0.569	ND	0.011	ND	ND
2.0	0.007	ND	ND	ND	0.915	ND	0.034	ND	ND
2.5	0.012	ND	ND	ND	1.295	ND	0.046	ND	ND
3.0	0.018	ND	ND	ND	1.546	ND	0.114	ND	ND

**Key:** ND = Not detected (below detection limit)

**XRD Results**

The mineralogical composition of Makukwa seep sediments is presented with X-ray diffractograms in **Figures 5 and 6**. From the Figures, Makukwa seep sediments are dominated by quartz. In each sampling area, the percentage composition of quartz was extremely high compared to other minerals. Quartz is a dominant mineral in sandstone formation (Xi et al., 2015), and its prevalence in the Makukwa seep sediments indicates the influence of sandstone in the sediment

composition. Graphite was observed in sampling area A than in sampling area B implying that area A has a high composition of hydrocarbons. Furthermore, it is observed that the seep sediments contain roquesite, larisate, rancidity, and porphyrazine aluminium chloride as minor mineralogical compositions in the seep sediment. These minerals occur as a fine-grained coating around the constituent grains, which are opaque to XRD (Ruff et al., 2015; Swayze et al., 2000). These minor minerals contribute to the overall mineralogical diversity of the seep

sediments, highlighting the complex nature of the sediment composition in this area.

The overall mineralogical profile, characterized by high quartz content along with traces of graphite and other minor minerals, provides crucial insights into the geological and geochemical framework of the Makukwa area. These findings are instrumental for hydrocarbon exploration as they suggest the potential for underlying sandstone reservoirs, which are favorable for oil and gas accumulation. The presence of graphite and other unique minerals also hints

at complex hydrocarbon maturation and migration processes, possibly influenced by historical thermal activities. These mineralogical indicators not only assist in pinpointing effective exploration targets but also raise important considerations for environmental monitoring and protection strategies. Understanding these implications helps in developing a comprehensive approach to managing both the exploration and environmental stewardship of the Makukwa seep region.

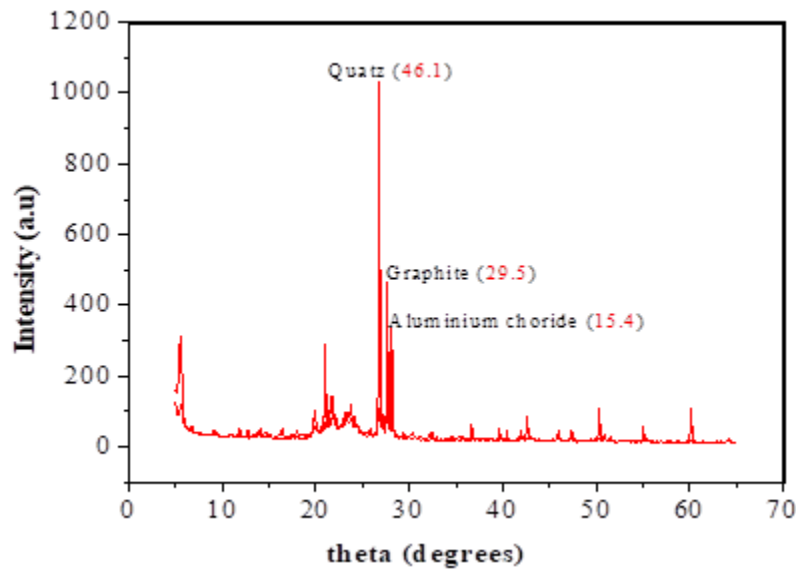


**Figure 5: X-ray Diffraction Patterns of Seep Sediment in Sampling Area A**

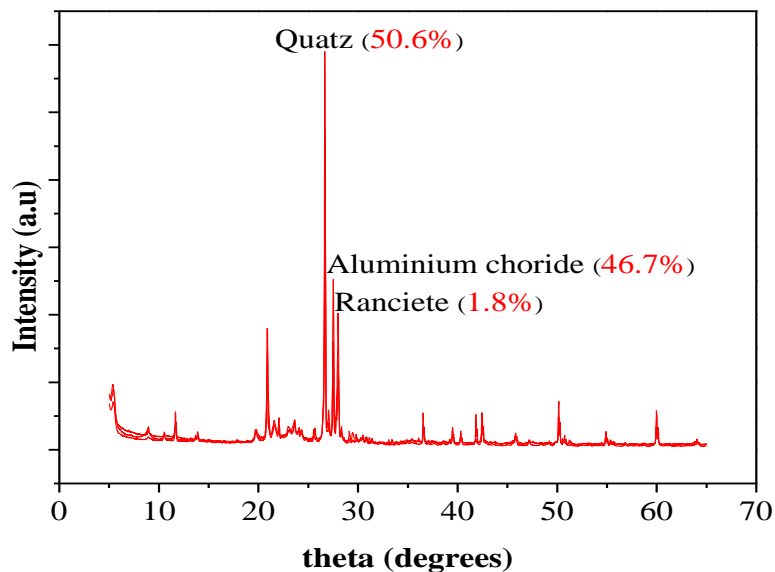


**Figure 6: X-ray Diffraction Patterns of Seep Sediment in Sampling Area B.**

## GC-MS Results: Hydrocarbon Profiles

The concentrations of hydrocarbons extracted from sediments as depicted in **Table 5** reveal the presence of aliphatic hydrocarbons, particularly n-alkanes ranging from n-C14 to n-C38, exhibiting both unimodal and bimodal distributions. Notably, the absence of lighter hydrocarbons in the seep sediment samples suggests inactive or minimal seepage activity, a condition that typically indicates a lesser or intermittent release of hydrocarbon gases from the subsurface. This aligns with findings reported in the literature, such as those by Kleindienst et al. (2012), which suggest that many hydrocarbon seeps are predominantly characterized by methane emissions, with other hydrocarbon gases present in only minor concentrations.

The variation in hydrocarbon concentrations between Area A and Area B, as highlighted in the results, suggests a spatial variance in seep activity or subsurface hydrocarbon reservoirs. Higher concentrations in Area A could likely be attributed to its closer proximity to an active seep pathway or a more direct connection to the subsurface hydrocarbon source. This makes Area A a more immediate recipient of seeping hydrocarbons, compared to Area B, which might be located further from the main seep source or shielded by geological formations that impede hydrocarbon migration.

The absence of light hydrocarbons and the presence of heavier alkanes may also be indicative of specific geochemical and biological processes. The lighter hydrocarbons, typically more volatile and biodegradable, are likely to have been either evaporated or metabolized by microbial activity prevalent in the sediment (Chakraborty et al., 2020; Lea-Smith et al., 2015). According to studies on marine hydrocarbon seep sediments, sulfate-reducing bacteria play a significant role in the biodegradation of alkanes, impacting the hydrocarbon profiles observed in such environments (Boruah et al., 2022; Stagars et al., 2016). These microbial communities are crucial in mediating the ecological impacts of

hydrocarbons, potentially transforming pollutants into less harmful substances. Furthermore, the role of environmental factors such as temperature, pressure, and sediment composition in affecting hydrocarbon solubility and migration patterns cannot be overlooked. These factors collectively influence the phase behavior of hydrocarbons, determining whether they remain trapped within the sediment or migrate towards the surface.

**Table 5: Hydrocarbon Composition of Makukwa Seep in Sampling Area A and Area B**

Compound name	Conc	Conc
	( $\mu\text{g/mL}$ ) Area A	( $\mu\text{g/mL}$ ) Area B
Tetradecane	–	0.058
Hexadecane	–	0.047
Octadecane	0.330	0.105
Nonadecane	0.239	–
Eicosane	0.789	0.089
Heneicosane	0.412	–
Docosane	–	0.056
Tetracosane	0.892	–
Pentacosane	0.761	–
Hexacosane	0.841	0.052
Heptacosane	0.816	0.048
Dotriacontane	0.129	–

## Results of the Physical and Chemical Properties of Extracted Hydrocarbons

The analysis of **Table 6** data on the physical and chemical properties of hydrocarbons extracted from areas A and B reveals low levels of sulfur content, ash content, and carbon residues. The composition of hydrocarbons, including sulfur content, influences the physicochemical properties of fuels, which in turn affect engine performance (Pradelle et al., 2016). The sulfur content below 0.002% in both areas is particularly noteworthy as sulfur compounds in hydrocarbons can lead to the formation of acidic by-products upon combustion, which are undesirable for both environmental and operational reasons. The minimal sulfur content suggests that the extracted

hydrocarbons are cleaner and would result in reduced emissions of sulfur dioxide when utilized as fuels (Sadeek et al., 2020; Yuan et al., 2022). Additionally, the presence of sulfur in hydrocarbons can perturb carbon and hydrogen retention levels, indicating the intricate relationship between sulfur and hydrocarbon characteristics (Warringham et al., 2020).

The ash content below 0.001% in the sampled hydrocarbons is advantageous as it indicates minimal inorganic matter, which can prevent operational issues like fouling and corrosion in engines and boilers (Elkasabi et al., 2015). Additionally, the low carbon residues of less than or equal to 0.01% suggest that these hydrocarbons would leave behind minimal

carbonaceous deposits upon combustion, aiding in maintaining the efficiency and longevity of combustion equipment (Ou et al., 2018; Sherwood Lollar et al., 2001). Moreover, the low carbon residues of less than or equal to 0.01% suggest that upon combustion, these hydrocarbons would leave behind minimal carbonaceous deposits, which is beneficial for maintaining the efficiency and longevity of combustion equipment (Freire et al., 2015; Zhao et al., 2013). These preliminary results provide a basis for further investigation into the economic potential and environmental benefits of these hydrocarbon sources, though more detailed studies are needed to fully establish these potentials.

**Table 6: Physical and Chemical Properties of Extracted Hydrocarbons**

Sampling Area	Properties	%wt Composition
A	Sulfur content	< 0.002
	Ash Content	< 0.001
	Carbon Residues	≤ 0.01
B	Sulfur content	< 0.002
	Ash Content	< 0.001
	Carbon Residues	≤ 0.01

## CONCLUSIONS AND RECOMMENDATIONS

This study provides a comprehensive analysis of the sediment physico-chemical properties and hydrocarbon composition at the Makukwa hydrocarbon seep in southern Tanzania. The study sheds light on the intricate relationship between geological formations and hydrocarbon seepage. Through meticulous sediment analysis, the porosity, mineral composition, and trace metal concentrations have been delineated alongside a detailed examination of the hydrocarbon spectrum present. Key findings include the porosity and particle size distribution, which suggest typical porosities of lower Cretaceous sandstone formations, with a noticeable decrease in porosity with depth due to compaction. Particle size distribution further supports the sandstone nature of the sediments. The elevated levels of trace metals, particularly iron, in sediments

near the seep suggest hydrocarbon-induced geochemical alterations. These findings highlight the significant influence of hydrocarbon seepage on sediment composition. XRD analysis identifies quartz as the dominant mineral, with variations in graphite content suggesting differential hydrocarbon influence across the sampled areas. GC-MS analysis reveals a range of heavy aliphatic hydrocarbons (n-alkanes) indicating a dormant state, with higher concentrations in sediments closer to the seep. The absence of lighter hydrocarbons points to minimal seepage activity and microbial degradation processes.

The implications of this study are far-reaching, offering theoretical and practical insights into geology and hydrocarbon exploration. The identification of specific geological formations associated with hydrocarbon seeps opens new avenues for targeted exploration efforts. Additionally, the study underscores the complexity of

subterranean hydrocarbon systems and the potential for leveraging sediment analysis to refine exploration techniques. Future research should focus on expanded investigations using advanced analytical technologies to validate these findings and explore broader implications for hydrocarbon exploration. Comprehensive geological surveys are essential to ascertain the extent of hydrocarbon-rich formations and their potential exploitation. The contributions of this research have significant potential for practical applications, influencing policy formulation and advancing theoretical frameworks within the field. By elucidating the sediment characteristics and hydrocarbon composition of the Makukwa seep in southern Tanzania, this study provides a critical foundation for future exploration strategies and enhances our understanding of subterranean hydrocarbon accumulation processes.

### Acknowledgements

The Tanzania Bureau of Standards is acknowledged for providing Claude A. Mosha with a scholarship that supported this research. Gratitude is also extended to the Chemistry Department, the School of Geosciences and Mining at the University of Dar es Salaam, and the Tanzania Bureau of Standards for granting access to their laboratories and equipment.

### Conflict of interest

The authors declare no competing conflict of interest regarding the publication of this research work.

### REFERENCES

Abrams, M. A. (2005). Significance of hydrocarbon seepage relative to petroleum generation and entrapment. *Marine and Petroleum Geology* **22**, 457-477.

Almeida-Filho, R., Miranda, F. P., and Yamakawa, T. (1999). Remote detection of a tonal anomaly in an area of hydrocarbon microseepage, Tucano basin, north-eastern Brazil. *International*

*Journal of Remote Sensing* **20**, 2683-2688.

Belzunce Segarra, M., Szefer, P., Wilson, M., Bacon, J., and Bolalek, J. (2007). Chemical forms and distribution of heavy metals in core sediments from the Gdańsk Basin, Baltic Sea. *Polish Journal of Environmental Studies* **16**.

Bohrmann, G. (2008). Report and preliminary results of R/V Meteor Cruise M74/3, Fujairah Male, 30 October-28 November, 2007. Cold Seeps of the Makran Subduction Zone (Continental Margin of Pakistan). *Berichte, Fachbereich Geowissenschaften, Universität Bremen*.

Boruah, A., Verma, S., Rasheed, A., Siddharth Gairola, G., and Gogoi, A. (2022). Macro-seepage based potential new hydrocarbon prospects in Assam-Arakan Basin, India. *Scientific Reports* **12**, 2273.

Carter, M. R., and Gregorich, E. G. (2007). "Soil sampling and methods of analysis," CRC press.

Cather, M., Morrow, N., and Klich, I. (1991). Characterization of porosity and pore quality in sedimentary rocks. In "Studies in surface science and catalysis", Vol. 62, pp. 727-736. Elsevier.

Chakraborty, A., Ruff, S. E., Dong, X., Ellefson, E. D., Li, C., Brooks, J. M., McBee, J., Bernard, B. B., and Hubert, C. R. (2020). Hydrocarbon seepage in the deep seabed links subsurface and seafloor biospheres. *Proceedings of the National Academy of Sciences* **117**, 11029-11037.

Ciotoli, G., Procesi, M., Etiope, G., Fracassi, U., and Ventura, G. (2020). Influence of tectonics on global scale distribution of geological methane emissions. *Nature Communications* **11**, 2305.

Clark, J. F., Washburn, L., and Schwager Emery, K. (2010). Variability of gas composition and flux intensity in natural marine hydrocarbon seeps. *Geo-Marine Letters* **30**, 379-388.

Cochran, J. K., Landman, N. H., Jakubowicz, M., Brezina, J., Naujokaityte, J., Rashkova, A., Garb, M. P., and Larson, N. L. (2022). Geochemistry of cold hydrocarbon seeps: an overview. *Ancient Hydrocarbon Seeps*, 3-45.

Dong, X., Zhang, T., Wu, W., Peng, Y., Liu, X., Han, Y., Chen, X., Gao, Z., Xia, J., and Shao, Z. (2024). A vast repertoire of secondary metabolites potentially

- influences community dynamics and biogeochemical processes in cold seeps. *Science Advances* **10**, ead12281-ead12281.
- Dupré, S., Woodside, J., Klaucke, I., Mascle, J., and Foucher, J.-P. (2010). Widespread active seepage activity on the Nile Deep Sea Fan (offshore Egypt) revealed by high-definition geophysical imagery. *Marine geology* **275**, 1-19.
- Elkasabi, Y., Mullen, C. A., and Boateng, A. A. (2015). Aqueous extractive upgrading of bio-oils created by tail-gas reactive pyrolysis to produce pure hydrocarbons and phenols. *ACS sustainable chemistry & engineering* **3**, 2809-2816.
- Freire, M., Lopes, H., and Tarelho, L. A. (2015). Critical aspects of biomass ashes utilization in soils: Composition, leachability, PAH and PCDD/F. *Waste management* **46**, 304-315.
- Ionescu, A., Burrato, P., Baciuc, C., Etiope, G., and Kis, B.-M. (2017). Inventory of onshore hydrocarbon seeps in Romania (HYSED-RO database). *Geosciences* **7**, 39.
- Japsen, P., Mukerji, T., and Mavko, G. (2007). Constraints on velocity-depth trends from rock physics models. *Geophysical Prospecting* **55**, 135-154.
- Joye, S. B. (2020). The geology and biogeochemistry of hydrocarbon seeps. *Annual review of earth and planetary sciences* **48**, 205-231.
- Kleindienst, S., Ramette, A., Amann, R., and Knittel, K. (2012). Distribution and in situ abundance of sulfate-reducing bacteria in diverse marine hydrocarbon seep sediments. *Environmental microbiology* **14**, 2689-2710.
- Laczkó-Dobos, E., Gier, S., Sztanó, O., Milovský, R., and Hips, K. (2020). Porosity development controlled by deep-burial diagenetic process in lacustrine sandstones deposited in a back-arc basin (Makó Trough, Pannonian Basin, Hungary). *Geofluids* **2020**, 1-26.
- Lahiri, S., Milliken, K. L., Vrolijk, P., Desbois, G., and Urai, J. L. (2022). Mechanical compaction mechanisms in the input sediments of the Sumatra Subduction Complex—insights from microstructural analysis of cores from IODP Expedition-362. *Solid Earth Discussions* **2022**, 1-47.
- Lai, J., Wang, G., Cai, C., Fan, Z., Wang, S., Chen, J., and Luo, G. (2018). Diagenesis and reservoir quality in tight gas sandstones: the fourth member of the Upper Triassic Xujiahe Formation, Central Sichuan Basin, Southwest China. *Geological Journal* **53**, 629-646.
- Lea-Smith, D. J., Biller, S. J., Davey, M. P., Cotton, C. A., Perez Sepulveda, B. M., Turchyn, A. V., Scanlan, D. J., Smith, A. G., Chisholm, S. W., and Howe, C. J. (2015). Contribution of cyanobacterial alkane production to the ocean hydrocarbon cycle. *Proceedings of the National Academy of Sciences* **112**, 13591-13596.
- Leifer, I., Melton, C., Manish, G., and Leen, B. (2014). Mobile monitoring of methane leakage. *Gases and Instrumentation* **2014**, 20-24.
- Li, A., Li, Q., Xu, C., Cai, F., and Wang, H. (2021). Review of methane seepages in the Okinawa trough: Progress and outlook. *Geofluids* **2021**, 1-13.
- Luo, D., Cai, F., Li, Q., Yan, G., Sun, Y., Li, A., and Dong, G. (2022). Geophysical evidence for submarine methane seepage on the Western slope of Okinawa Trough. *Frontiers in Earth Science* **10**, 985597.
- Mishra, A. K., Santos, R., and Hall-Spencer, J. (2020). Elevated trace elements in sediments and seagrasses at CO<sub>2</sub> seeps. *Marine environmental research* **153**, 104810.
- Muhongo, S. (2013a). Tanzania as an emerging energy producer. Africa meeting summary. Chatham house, London.
- Muhongo, S. (2021). Local Content Policies in the Energy Transition Era in Africa: A Case Study of the East African Oil and Gas Industry. *Energy Transitions and the Future of the African Energy Sector: Law, Policy and Governance*, 311-340.
- Muhongo, S. M. (2013b). The National Natural Gas Policy of Tanzania - 2013. *Ministry of Energy and Minerals*.
- Ou, L., Kim, H., Kelley, S., and Park, S. (2018). Impacts of feedstock properties on the process economics of fast-pyrolysis biorefineries. *Biofuels, Bioproducts and Biorefining* **12**, 442-452.
- Pradelle, F., Leal Braga, S., Fonseca de Aguiar Martins, A. R., Turkovics, F., and Nohra Chaar Pradelle, R. (2016). Modeling of unwashed and washed gum content in Brazilian gasoline–ethanol blends during prolonged storage: application of a

- Doehlert matrix. *Energy & Fuels* **30**, 6381-6394.
- Rachel Angelo, S., Ehinola, O., Mtelela, C., and Edwin Ayuk, N. (2019). Intergrated Seismic Stratigraphic and Structural Analysis of the Songo Songo Gas-Field, Shallow Offshore Tanzania, Using Seismic and Well Data. *J Geol Geophys* **8**, 2.
- Rasheed, M., Lakshmi, M., Rao, P., Kalpana, M., Dayal, A., and Patil, D. (2013). Geochemical evidences of trace metal anomalies for finding hydrocarbon microseepage in the petroliferous regions of the Tatipaka and Pasarlapudi areas of Krishna Godavari Basin, India. *Petroleum Science* **10**, 19-29.
- Ruff, S. E., Biddle, J. F., Teske, A. P., Knittel, K., Boetius, A., and Ramette, A. (2015). Global dispersion and local diversification of the methane seep microbiome. *Proceedings of the National Academy of Sciences* **112**, 4015-4020.
- Sadeek, S. A., Mohammed, E. A., Shaban, M., Abou Kana, M. T., and Negm, N. A. (2020). Synthesis, characterization and catalytic performances of activated carbon-doped transition metals during biofuel production from waste cooking oils. *Journal of Molecular Liquids* **306**, 112749.
- Schumacher, D., and Foote, R. S. (2014). Seepage-induced magnetic anomalies associated with oil and gas fields: onshore and offshore examples. In "AAPG International Conference and Exhibition", Istanbul, Turkey.
- Sherwood Lollar, B., Slater, G. F., Sleep, B., Witt, M., Klecka, G., Harkness, M., and Spivack, J. (2001). Stable carbon isotope evidence for intrinsic bioremediation of tetrachloroethene and trichloroethene at area 6, Dover Air Force Base. *Environmental science & technology* **35**, 261-269.
- Stagars, M. H., Ruff, S. E., Amann, R., and Knittel, K. (2016). High diversity of anaerobic alkane-degrading microbial communities in marine seep sediments based on (1-methylalkyl) succinate synthase genes. *Frontiers in microbiology* **6**, 152722.
- Swayze, G. A., Smith, K. S., Clark, R. N., Sutley, S. J., Pearson, R. M., Vance, J. S., Hageman, P. L., Briggs, P. H., Meier, A. L., and Singleton, M. J. (2000). Using imaging spectroscopy to map acidic mine waste. *Environmental Science & Technology* **34**, 47-54.
- Techtmann, S. M., Fortney, J. L., Ayers, K. A., Joyner, D. C., Linley, T. D., Pfiffner, S. M., and Hazen, T. C. (2015). The unique chemistry of Eastern Mediterranean water masses selects for distinct microbial communities by depth. *PLoS One* **10**, e0120605.
- TPDC, T. P. D. C. (1992). "Petroleum potential of Tanzania."
- USEPA (2016). National rivers and streams assessment 2008-2009 technical report. EPA 841/R-16/008.
- Wang, X., Jiang, Z., Jiang, S., Chang, J., Li, X., Wang, X., and Zhu, L. (2019). Pore evolution and formation mechanism of organic-rich shales in the whole process of hydrocarbon generation: study of artificial and natural shale samples. *Energy & fuels* **34**, 332-347.
- Ward, C. H., Byrnes, M. R., Rowe, G. T., Davis, R. A., and Tunnell, J. W. (2017). "Water quality, sediments, sediment contaminants, oil and gas seeps, coastal habitats, offshore plankton and benthos, and shellfish," Springer Nature.
- Warringham, R., Davidson, A. L., Webb, P. B., Tooze, R. P., Parker, S. F., and Lennon, D. (2020). Perspectives on the effect of sulfur on the hydrocarbonaceous overlayer on iron Fischer-Tropsch catalysts. *Catalysis Today* **339**, 32-39.
- Xi, K., Cao, Y., Jahren, J., Zhu, R., Bjørlykke, K., Zhang, X., Cai, L., and Hellevang, H. (2015). Quartz cement and its origin in tight sandstone reservoirs of the Cretaceous Quantou formation in the southern Songliao basin, China. *Marine and Petroleum Geology* **66**, 748-763.
- Yuan, S., Zhang, Y., Wan, Z., Yin, H., and Chen, Z. (2022). Study on the Reactive Extraction Process for Heptaldehyde–Undecane–Sodium Bisulfite Aqueous Solution System. *Industrial & Engineering Chemistry Research* **61**, 9422-9432.
- Zhao, M., Han, Z., Sheng, C., and Wu, H. (2013). Characterization of residual carbon in fly ashes from power plants firing biomass. *Energy & fuels* **27**, 898-907.